

RESEARCH

Open Access



An image cytometric technique is a concise method to detect adenoviruses and host cell proteins and to monitor the infection and cellular responses induced

Takao Morinaga¹, Thảo Thi Thanh Nguyễn^{1,2}, Boya Zhong^{1,2}, Michiko Hanazono¹, Masato Shingyoji³, Ikuo Sekine⁴, Yuji Tada⁵, Koichiro Tatsumi⁵, Hideaki Shimada⁶, Kenzo Hiroshima⁷ and Masatoshi Tagawa^{1,2*}

Abstract

Background: Genetically modified adenoviruses (Ad) with preferential replications in tumor cells have been examined for a possible clinical applicability as an anti-cancer agent. A simple method to detect viral and cellular proteins is valuable to monitor the viral infections and to predict the Ad-mediated cytotoxicity.

Methods: We used type 5 Ad in which the expression of *E1A* gene was activated by 5'-regulatory sequences of genes that were augmented in the expression in human tumors. The Ad were further modified to have the fiber-knob region replaced with that derived from type 35 Ad. We infected human mesothelioma cells with the fiber-replaced Ad, and sequentially examined cytotoxic processes together with an expression level of the viral E1A, hexon, and cellular cleaved caspase-3 with image cytometric and Western blot analyses.

Results: The replication-competent Ad produced cytotoxicity on mesothelioma cells. The infected cells expressed E1A and hexon 24 h after the infection and then showed cleavage of caspase-3, all of which were detected with image cytometry and Western blot analysis. Image cytometry furthermore demonstrated that increased Ad doses did not enhance an expression level of E1A and hexon in an individual cell and that caspase-3-cleaved cells were found more frequently in hexon-positive cells than in E1A-positive cells. Image cytometry thus detected these molecular changes in a sensitive manner and at a single cell level. We also showed that an image cytometric technique detected expression changes of other host cell proteins, cyclin-E and phosphorylated histone H3 at a single cell level.

Conclusions: Image cytometry is a concise procedure to detect expression changes of Ad and host cell proteins at a single cell level, and is useful to analyze molecular events after the infection.

Keywords: Replication-competent adenovirus, Image cytometry, E1A, Hexon, Cleaved caspase-3

Background

Recombinant replication-competent viruses were demonstrated to produce cytotoxic effects preferentially on tumors and a number of clinical trials were conducted to evaluate efficacy and safety of the viral agents [1]. Herpes simplex viruses expressing *granulocyte macrophage colony stimulating factor* gene, for example,

produced significant effects on metastatic melanoma and have been approved in USA and EU [2]. Adenoviruses (Ad) are one of the agents that are relatively easy to be genetically modified and are commonly used to produce replication-restricted types targeting human tumors. Preferential Ad replication in tumors can be achieved by activation of the E1A region with a transcriptional regulatory unit of a gene which is up-regulated in human tumors [3]. Replacing an authentic viral E1A regulatory region with such an exogenous region enable Ad to proliferate in tumors without damaging normal tissues and consequently tumor cell death

* Correspondence: mtagawa@chiba-cc.jp

¹Division of Pathology and Cell Therapy, Chiba Cancer Center Research Institute, 666-2 Nitona, Chuo-ku, Chiba 260-8717, Japan

²Department of Molecular Biology and Oncology, Graduate School of Medicine, Chiba University, Chiba, Japan

Full list of author information is available at the end of the article



was induced. We and others previously showed that a 5' untranslated region of *survivin* (Sur) [4] or *midkine* (MK) [5] gene, which were up-regulated in the expression in a number of human tumors, activated a reporter gene in human tumors but much less in human normal cells. Replication-competent Ad powered by such a regulatory region in fact produced cytotoxicity in various type of human tumors [4, 6]. We also developed Ad in which the fiber-knob region, mediating Ad binding to the cellular receptors [7], was replaced with that of other subtypes. Type 5 Ad use coxsachie adenovirus receptor (CAR) as the main cellular receptor and integrin $\alpha\beta 3$ and $\alpha\beta 5$ as the ancillary receptor, whereas type 35 Ad vector use CD46 as the main receptor [8]. Type 5 Ad bearing the Ad35-derived fiber-knob structure (AdF35) therefore infected CD46-positive cells irrespective of CAR expression [9, 10]. An expression level of CAR molecules in human tumors is often down-regulated, whereas that of CD46 molecules was rather up-regulated in a number of human tumors [11]. AdF35 consequently infected human tumors better than Ad5 [12] and produced greater cytotoxicity [13].

A mechanism of cell death induced by Ad replications can be different from that by conventional chemotherapy. Replication-competent Ad were thereby examined for a possible combinatory use with the anti-cancer agents and recently with immunotherapy [14]. Prediction of Ad-mediated cytotoxicity will be important in a future clinical application but such a predictive biomarker remains unknown in a preclinical study. One of the reasons is a complexity of Ad-mediated cell death since viral replications and subsequent viral spreading are influenced by cellular factors which may affect infection efficacy in an interaction between tumor cells and the microenvironment, anti-viral immune responses and susceptibility of tumors to cell death [15, 16].

Detailed analyses of viral and cellular proteins expressed are crucial for investigating viral replications and induction of cytotoxicity in target cells. Western blot analysis can show expression levels of viral and cellular proteins in a population but is not be suitable for detecting those in a small cell population. In this study, we tested a possible use of image cytometry by detecting the viral early and late proteins together with cellular proteins. Image cytometry can analyze gene expression and the levels of multiple proteins with easy. The present study demonstrated that an image cytometric technique was a handy method to monitor expression of viral and host cell proteins at a single cell level.

Methods

Cells

Human mesothelioma, NCI-H2452 and MSTO-211H cells, and a packaging cell line for Ad production,

HEK293 cells, were purchased from ATCC (Manassas, VA, USA) and were cultured with RPMI 1640 supplemented with 10% fetal calf serum and penicillin/streptomycin (P4333, Merck, St. Louis, MO, USA) under 5% CO₂ in air at 37 °C.

Construction of Ad

AdF35 DNA were produced with the Adeno-X vector (type 5 Ad, Takara, Shiga, Japan) in which the fiber-knob region (accession number: M73260 at 31042-32787) was replaced with that of Ad35 DNA (Avior Therapeutic, Seattle, WA, USA) [17]. Replication-competent AdF35 in which the *E1* gene was activated by an exogenous regulatory element of survivin (AdF35/Sur) or midkine (AdF35/MK) were prepared by replacing the authentic E1 promoter region with 5'-upstream regulatory sequences of the *Sur* (0.5 kb, U75285) [4] or the *MK* (0.6 kb, D10604) [5] gene. Replication-incompetent AdF35 expressing the β -galactosidase gene (NM066611) activated by cytomegalovirus promoter (BK000394) (AdF35/LacZ) were prepared with the above Adeno-X vector which were partly replaced with Ad35 DNA [17]. The above Ad DNA was transfected into HEK293 cells and Ad produced were purified with an Adeno-X virus purification kit (Takara) (Additional file 1). The numbers of virus particles (vp) per ml was estimated with the formula, absorbance at 260 nm of purified Ad in the presence of 0.1% sodium dodecyl sulfate $\times 1.1 \times 10^{12}$ [18].

Ad infection

Cells (1.6×10^5 cells/ml, 3×10^4 cells/cm²) were seeded on tissue-culture grade dishes (353,002, Corning, NY, USA) a day before infection. Ad stock solutions (AdF35/Sur; 1.2×10^{12} vp/ml, AdF35/MK; 2.5×10^{12} vp/ml, Ad35/LacZ; 1.2×10^{12} vp/ml) were diluted with 4 ml of RPMI1640 with 10% fetal calf serum to final virus concentrations depending on respective experiments. Culture medium was then completely replaced with the Ad-containing medium and cells were further cultured for the time indicated. For cytotoxicity test with a dye exclusion assay, cells (2.0×10^4 cells/ml, 4.2×10^3 cells/cm²) were seeded on 6-well cell culture plate (353,046, Corning) a day before infection. Ad stock solutions were diluted with 2 ml of RPMI1640 with 10% fetal calf serum to final virus concentrations (10^4 vp/cell). Infection was performed as above.

Cytotoxicity of Ad

Infection of cells with Ad was performed by adding Ad onto cells in cell culture and numbers of cells infected with AdF35/Sur were counted with the trypan blue dye exclusion assay [19]. The adherent and floating cells were also counted.

Immunofluorescence

Cells infected with AdF35/Sur were sequentially treated with 2% paraformaldehyde for 15 min, 0.2% Triton X-100 for 5 min, and 0.1% saponin/3% bovine serum albumin for 30 min. The cells were incubated with anti-Ad type 2/5 E1A antibody (Ab) (sc-25, 1: 50 dilution, Santa Cruz Biotech, Dallas, TX, USA) followed by anti-mouse IgG labeled with Alexa Fluor 488 (A-21202, 1: 500, Thermo Fisher Scientific, Fremont, CA, USA) and RNase A (200 µg/ml) for 1 h. They were further treated with propidium iodide (50 µg/ml) for 30 min for nuclear visualization with a confocal laser microscope, Leica TCS SP8 with a 40× Oil-immersion objective lens (Leica microsystems, Deerfield, Illinois, USA).

Image cytometry

Cells infected with AdF35/Sur were sequentially treated with 2% paraformaldehyde for 15 min, 0.2% Triton X-100 for 5 min, and 0.1% saponin/3% bovine serum albumin for 30 min. The cells were then incubated with Ab against Ad type 2/5 E1A (1: 50) or Ad hexon E11 (sc-52,365, 1: 50, Santa Cruz Biotech), and with cleaved caspase-3 (#9664S, 1: 200, Cell Signaling, Danvers, MA, USA) for 1 h, followed by anti-mouse IgG labeled with Alexa Fluor 488 (1: 500) or anti-rabbit IgG labeled with Alexa Fluor 555 (ab150074, 1: 500, Abcam, Cambridge, UK) for 1 h. They were analyzed with Tali image-based cytometer (Thermo Fisher Scientific, Fremont, CA, USA).

Western blot analysis

Cells were lysed with a buffer containing 2% sodium dodecyl sulfate with protease inhibitor cocktail (P8340, Merck), phosphatase inhibitor cocktail solution I (167-24,381, Wako, Osaka, Japan), 0.5 mM EDTA and 5% 2-mercaptoethanol, and were sonicated. Lysate of MSTO-211H cells infected with AdF35/Sur was subjected to sodium dodecyl sulfate polyacrylamide gel electrophoresis [20]. The protein was transferred to a nylon filter and was hybridized with Ab against Ad type 2/5 E1A (1: 200), hexon (1: 200), pRb (#9309, 1: 1000), cleaved caspase-3 (Cell Signaling, 1: 1000), γ -H2A histone family member X (γ -H2AX) (#613401, BioLegend, San Diego, CA, USA, 1: 500), NBS-1 (ab23996, Abcam, 1: 1000), p53 (Ab-6, Clone DO-10, 1: 1600), or tubulin- α (DMIA, Thermo Fisher Scientific, 1:3000) as a loading control. The membranes were developed with the ECL system (GE Healthcare, Buckinghamshire, UK).

Results

AdF35/Sur-mediated cytotoxicity

We examined cytotoxic effects of AdF35/Sur on human mesothelioma, MSTO-211H cells with the wild-type *p53* genotype (Fig. 1). Cells infected with AdF35/Sur became detached from a culture plate and floated in a dose-

dependent manner (Fig. 1a). Growth of AdF35/Sur-infected cells were retarded although they were not dead until day 3 (Fig. 1b). The cell numbers then decreased on day 6, indicating that cell death was induced. In contrast, proliferation of AdF35/LacZ-infected cells were minimally suppressed.

An immunofluorescent staining showed that Ad early protein, E1A, was expressed in the nuclei on day 1 (Fig. 1c). We detected expression of E1A from 24 h and that of hexon, one of the Ad late genes, from 48 h after the infection with Western blot analysis (Fig. 1d). We also detected cleavage of caspase-3 from 48 h. These data indicated sequential expression of Ad early gene and late gene products followed by an apoptotic process. AdF35/Sur infection also induced γ -H2AX expression, a DNA damage marker, at 24 h, and expression of NBS-1, a marker for cellular DNA damage responses, was down-regulated upon Ad infection as reported [21]. Furthermore, p53 expression increased due to Ad-induced DNA damages, and pRb expression decreased thereafter.

Detection of E1A and cleaved caspase-3 with image cytometry

We examined a possible use of image cytometry to detect E1A and cleaved caspase-3 at a single cell level (Fig. 2). A dual staining with anti-E1A and anti-cleaved caspase-3 Ab showed that E1A expression was detected as early as 12 h after the infection, significantly augmented at 24 h and decreased thereafter (Fig. 2a & b). In contrast, cleaved caspase-3 was detected even in untreated cells and the cleavage in infected cells increased after 48 h. Double positive cells for E1A and cleaved caspase-3 were minimally detected. We also examined E1A expression at 24 h with Western blot analysis under the same experimental condition as used in the image cytometric analysis (Fig. 2c). The E1A expression increased in an Ad dose-dependent manner but was scarcely detected in cells infected at 10^3 vp/cell in contrast to image cytometry which detected E1A-positive cells infected at the same dose. These data collectively indicated that image cytometry enabled us to detect E1A with increased sensitivity. We also calculated an average E1A intensity of the positively stained cells which were infected at 10^3 or 10^4 vp/cell (Fig. 2d). The intensity of cells infected at 10^3 vp/cell was different only at 48 h from that of those at 10^4 vp/cell although the positive cell numbers were greater in infection at 10^4 vp/cell than in that at 10^3 vp/cell. A range of the E1A expression level per cell was thus similar irrespective of Ad doses. Increase of E1A expression according to Ad doses, detected with Western blot analysis, was therefore attributable to increased numbers of infected cells but not to an enhanced E1A expression level per cell.

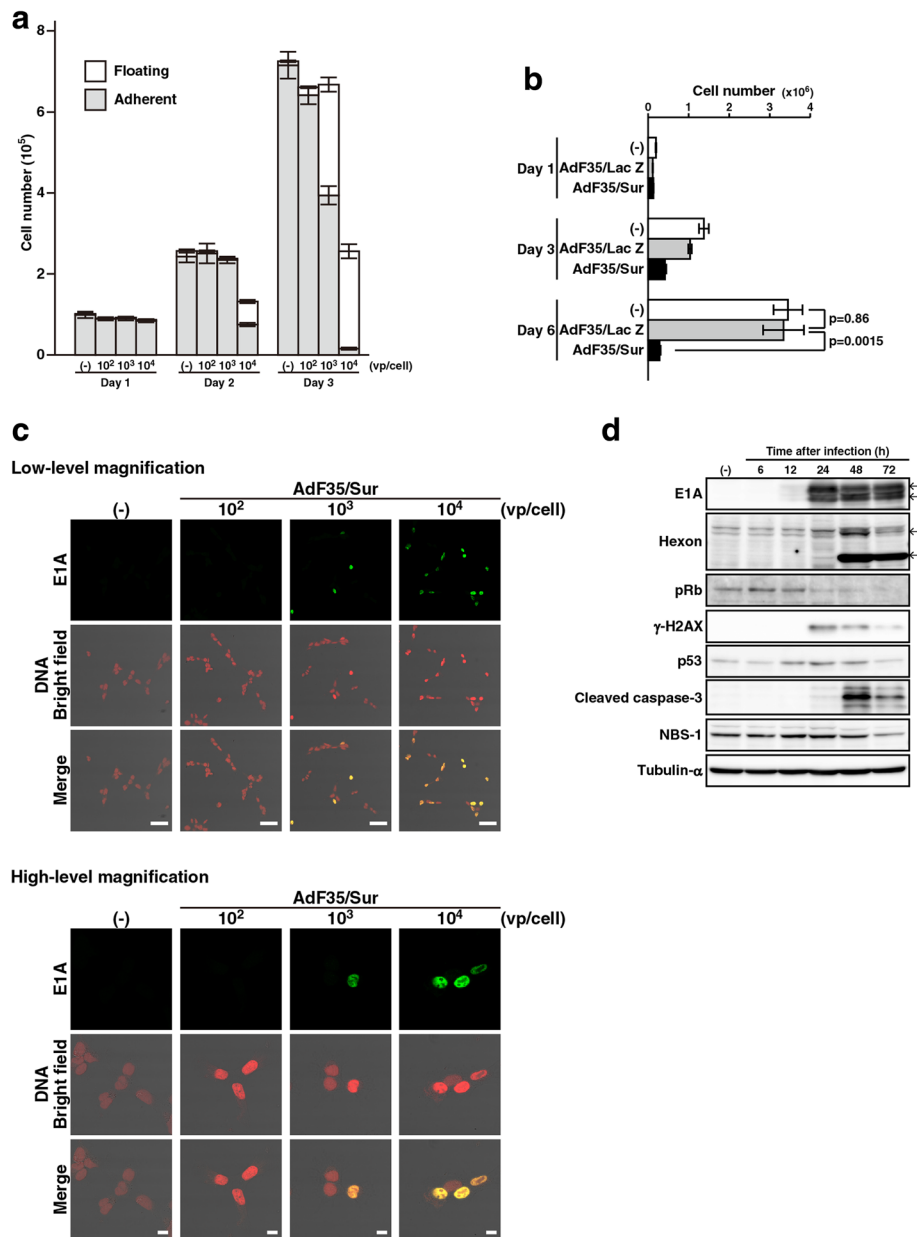


Fig. 1 AdF35/Sur-mediated cytotoxicity. **a** MSTO-211H cells were uninfected or infected with AdF35/Sur at a vp/cell dose as indicated, and the numbers of adherent and floating cells were counted. Average and SE bars are shown. (-): uninfected. **b** MSTO-211H cells were uninfected or infected with AdF35/LacZ or AdF35/Sur (10^4 vp/cell) and live cell numbers were counted with a trypan blue dye exclusion assay. **c** MSTO-211H cells were uninfected or infected with AdF35/Sur at a vp/cell as indicated for 1 day, and were stained with anti-E1A Ab and propidium iodide. **d** MSTO-211H cells were uninfected or infected with AdF35/Sur (10^4 vp/cell) as indicated and were examined for the expression levels of viral and cellular proteins with Western blot analysis. E1A and hexon showed multiple bands. Tubulin- α was used as a loading control

Detection of hexon and cleaved caspase-3 with image cytometry

We then stained AdF35/Sur-infected cells with Ab against hexon and cleaved caspase-3 (Fig. 3a). Expression of hexon was detected after 24 h and reached to the maximum at 48 h (Fig. 3b). Cleaved caspase-3 expression was not different from the expression of cells stained dually with anti-E1A Ab (Fig. 2a). Percentages

of the cell population positive for both hexon and cleaved caspase-3 were greater than those of double positive cells for E1A and cleaved caspase-3, indicating that caspase-3 was cleaved in a later phase of Ad infection. Interestingly, an expression level of hexon per cell was greater in infection at 10^3 vp/cell than in infection at 10^4 vp/cell (Fig. 3c). The hexon level was thus not correlated with virus dose used and these

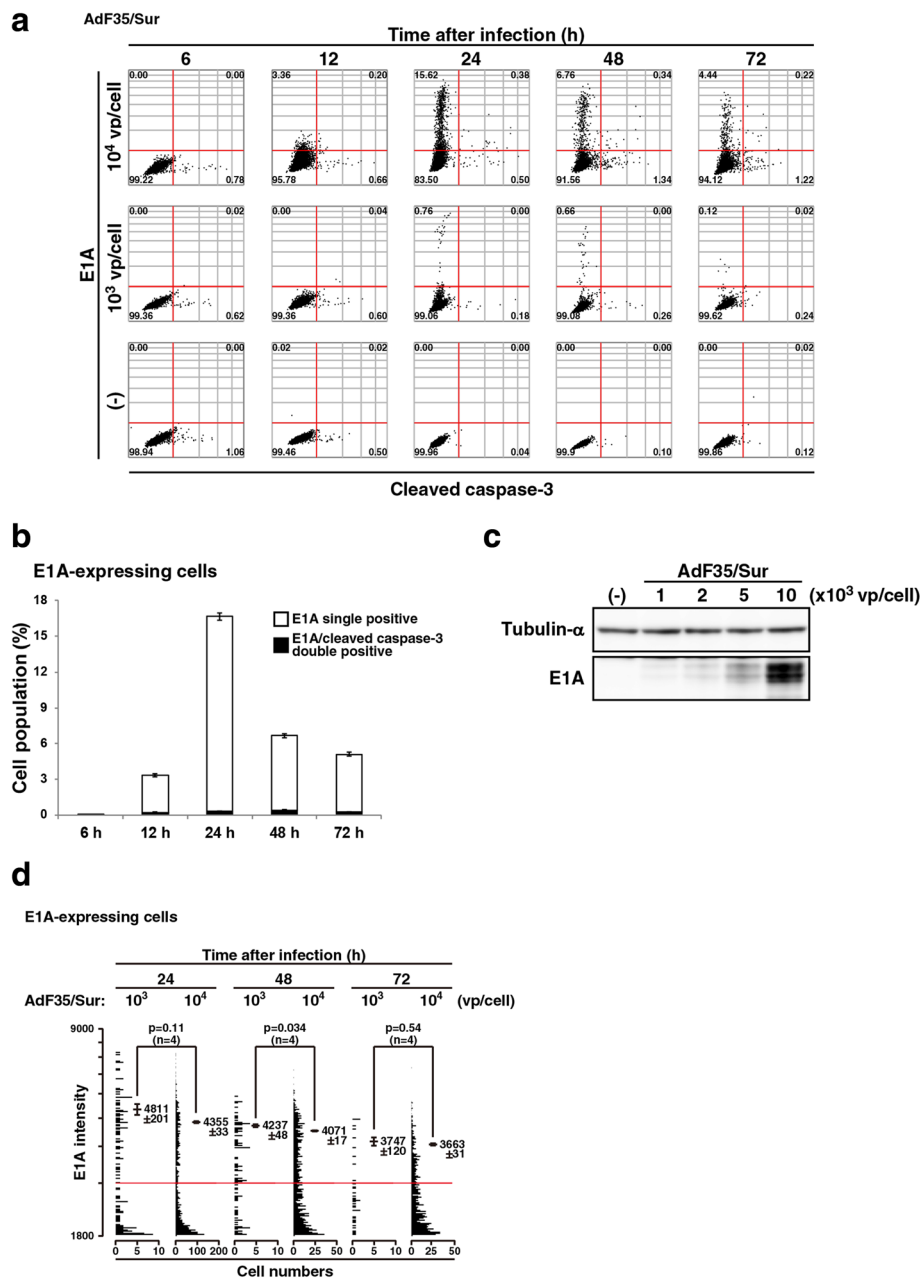
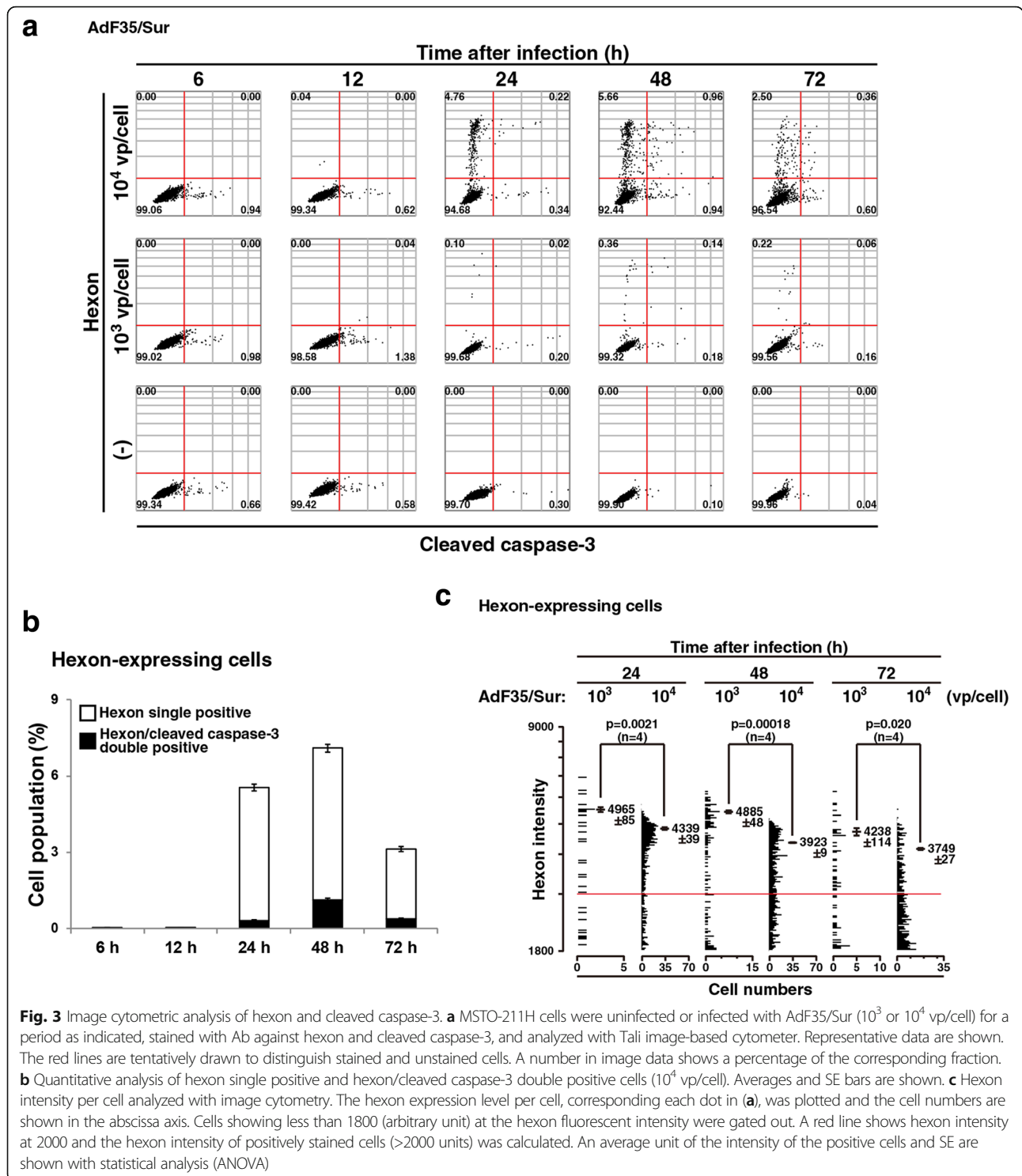


Fig. 2 Image cytometric analysis of E1A and cleaved caspase-3. **a** MSTO-211H cells were uninfected or infected with AdF35/Sur (10^3 or 10^4 vp/cell) for a period as indicated, stained with Ab against E1A and cleaved caspase-3, and analyzed with Tali image-based cytometer. Representative data are shown. The red lines are tentatively drawn to distinguish stained and unstained cells. A number in image data shows a percentage of the corresponding fraction. **b** Quantitative analysis of E1A single positive and E1A/cleaved caspase-3 double positive cells (10^4 vp/cell). Averages and SE bars are shown. **c** Western blot analysis to detect E1A expression in MSTO-211H cells uninfected or infected with AdF35/Sur at a vp/cell dose as indicated for 24 h. (-): uninfected. **d** E1A intensity per cell analyzed with image cytometry. The E1A expression per cell, corresponding each dot in (a), was plotted and the dot numbers are shown in the abscissa axis. Cells showing less than 1800 (arbitrary unit) at the E1A fluorescent intensity were gated out. A red line shows E1A intensity at 2000 and the E1A intensity of positively stained cells (>2000 units) was calculated. An average unit of the intensity of the positive cells and SE are shown with statistical analysis (ANOVA)

data indicated that infection with a high dose of Ad increased numbers of infected cells but did not augment an expression level of the viral genes per cell.

Feasibility of image cytometric detection

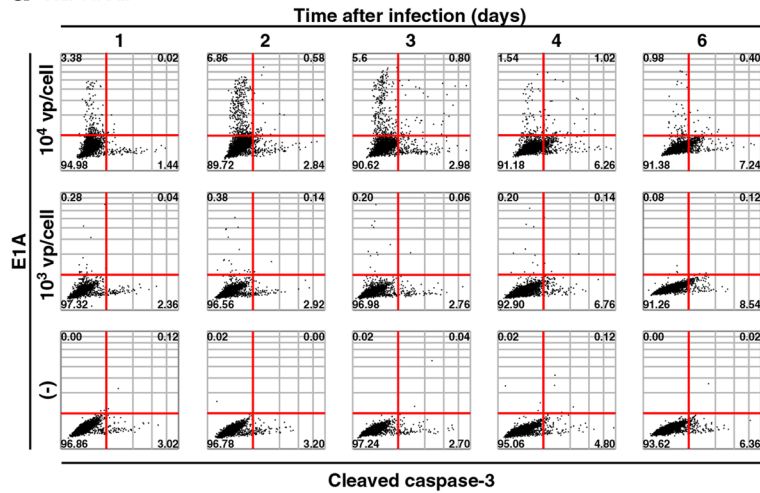
We further examined feasibility of image cytometric detection with different cells and replication-competent Ad (Fig. 4). Human mesothelioma NCI-H2452 cells were



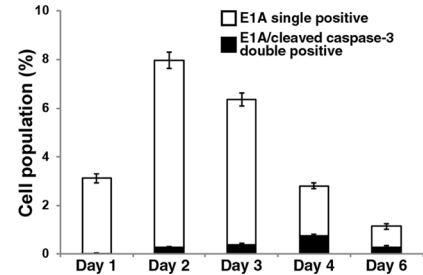
infected with AdF35/Sur and examined for expression of E1A and hexon together with cleaved caspase-3 (Fig. 4a & b). NCI-H2452 cells had a truncated p53 protein [22] and were relatively resistant to Ad-mediated cytotoxicity. We then examined the expression levels until day 6. Expression of E1A reached to the maximum level on day 2

and decreased thereafter (Fig. 4a). Hexon expression became the highest on day 3 and the level declined thereafter. A dual staining with cleaved caspase-3 demonstrated that cells positive for both E1A and cleaved caspase-3 was few than those positive for hexon and cleaved caspase-3. These data indicated that AdF35/

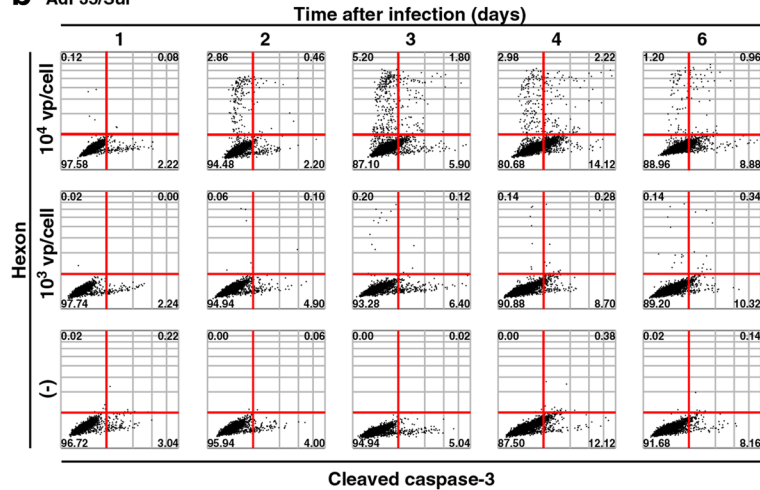
a AdF35/Sur



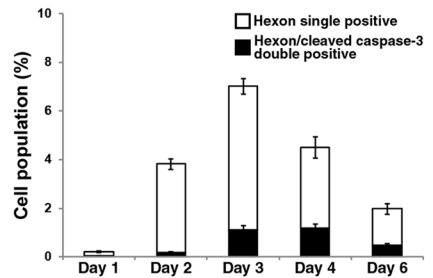
E1A-expressing cells



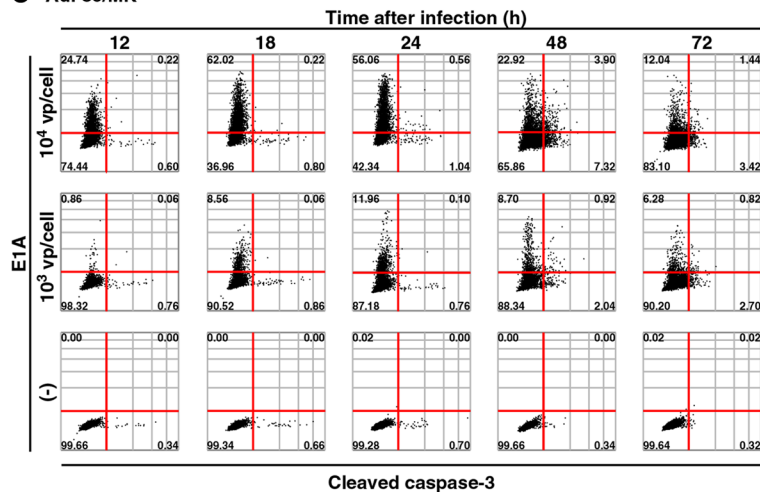
b AdF35/Sur



Hexon-expressing cells



c AdF35/MK



E1A-expressing cells

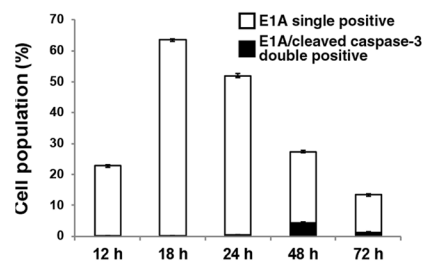


Fig. 4 (See legend on next page.)

(See figure on previous page.)

Fig. 4 Image cytometric analysis of viral and cellular proteins. **a** NCI-H2452 cells were uninfected or infected with AdF35/Sur (10^3 or 10^4 vp/cell) for a period as indicated, stained with Ab against E1A and cleaved caspase-3, and analyzed with Tali image-based cytometer. Representative data are shown. The red lines are tentatively drawn to distinguish stained and unstained cells. A number in image data shows a percentage of the corresponding fraction. (-): uninfected. Bar graphs shows quantitative analysis of E1A single positive and E1A/cleaved caspase-3 double positive cells in **(a)** (10^4 vp/cell). Averages and SE bars are shown. **b** NCI-H2452 cells were infected as shown in **(a)** and stained with Ab against hexon and cleaved caspase-3. Bar graph shows quantitative analysis of hexon single positive and hexon/cleaved caspase-3 double positive cells in **(b)** (10^4 vp/cell). **c** MSTO-211H cells were uninfected or infected with AdF35/MK (10^3 or 10^4 vp/cell) for a period as indicated, stained with Ab against E1A and cleaved caspase-3, and analyzed with Tali image-based cytometer. Bar graph shows quantitative analysis of E1A single positive and E1A/cleaved caspase-3 double positive cells in **(c)** (10^4 vp/cell)

Sur-induced expression profiles of viral and cellular proteins were similar between MSTO-211H cells and NCI-H2452 cells although time to attain the maximum expression was different.

We next tested E1A and cleaved caspase-3 expression levels in MSTO-211H cells infected with a different type of replication-competent Ad, AdF35/MK (Fig. 4c). E1A was detected 12 h after the infection and the expression reached at the maximum at 18 h, whereas cells positive for cleaved caspase-3 became maximum at 48 h in infection at 10^4 vp/cell. These expression profiles were relatively similar to those of MSTO-211H cells infected

with AdF35/Sur although a differential transcriptional activity between the *Sur* and the *MK* gene might influence the viral gene expression.

We also examined expression of cyclin E and phosphorylated histone H3 in combination with E1A expression with image cytometry (Fig. 5a). Ad infection facilitated S-phase entry and M-phase exit in cell cycle and we used cyclin E and phosphorylated histone H3 as a maker for S-phase and M-phase, respectively [23, 24]. MSTO-211H cells significantly increased percentages of cyclin E-positive cells 2 days after AdF35/Sur infection (uninfected cells; $0.9 \pm 0.09\%$, infected cells;

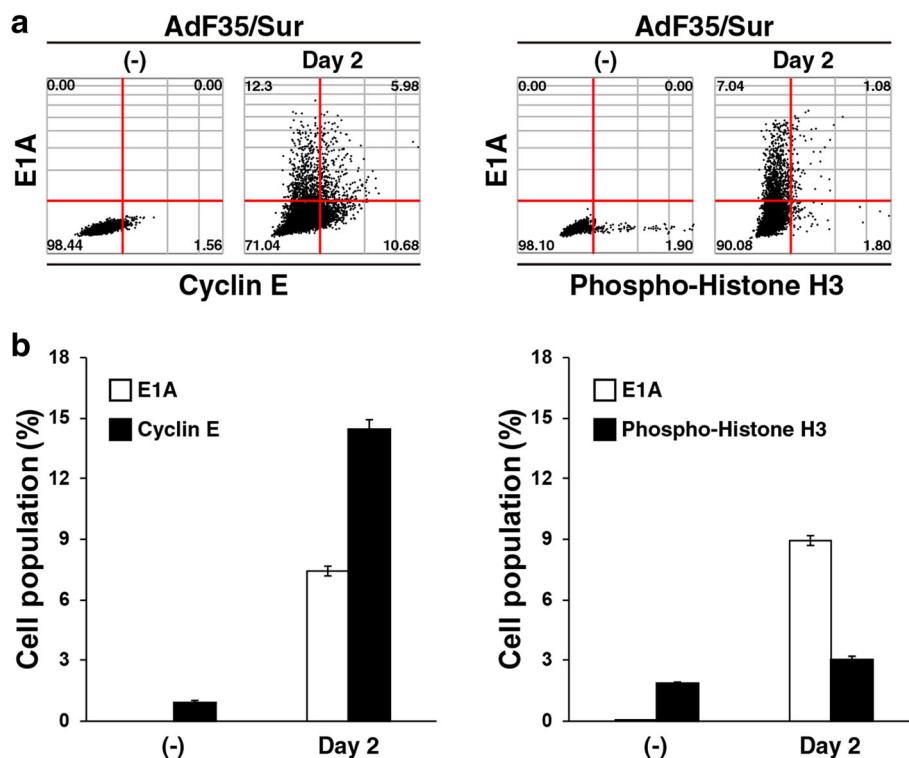


Fig. 5 Image cytometric analysis of cellular proteins. **a** MSTO-211H cells were uninfected or infected with AdF35/Sur (10^4 vp/cell), stained with Ab against cyclin E or phosphorylated histone H3 and E1A, and analyzed with Tali image-based cytometer. Representative data are shown. The red lines are tentatively drawn to distinguish stained and unstained cells. A number in image data shows a percentage of the corresponding fraction. (-): uninfected. **b** Quantitative analysis of E1A-, cyclin E- and phosphorylated histone H3-positive cells in **(a)**. Averages and SE bars are shown

14.4 + 0.52%), whereas those marginally increased percentages of cells positive for phosphorylated histone H3 (uninfected cells; 1.9 + 0.07%, infected cells; 3.0 + 0.18%), (Fig. 5b). These data were consistent with the previous studies [23, 24] and demonstrated that an image cytometric analysis detected viral and cellular proteins at a single cell level.

Discussion

We investigated a possible image cytometric analysis of Ad early and late proteins together with cellular proteins. An image cytometry technique detected Ad proteins, E1A and hexon molecules, and cellular proteins, cleaved caspase-3, cyclin E and phosphorylated histone H3 molecules, at a single cell level. The technique is concise with less amounts of cells required in comparison with Western blot analysis and enables us to investigate molecular expression profiles quantitatively.

We detected E1A expression in cells infected with replication-competent Ad and compared detection sensitivity between image flow cytometer and Western blot analysis with the same Ab. We may not be able to conclude differential sensitivity since a detection level is influenced by many factors including affinity of the second Ab used. Nevertheless, an image cytometry technique could detect a small fraction of Ad-infected population as being E1A-positive in contrast to Western blot analysis that detected the E1A level in a whole cell population infected with a high Ad dose. We can therefore conclude that an image cytometric analysis is more sensitive to detect viral proteins than Western blot analysis. We also analyzed hexon, one of the Ad major proteins, and cleaved caspase-3, cellular protein involved in apoptosis, and demonstrated that E1A expression preceded hexon expression and cleaved caspase-3 was expressed preferentially in hexon-positive cells rather than E1A-positive cells. These data are quite understandable in terms of Ad replication processes. We also noticed that a range of an E1A or a hexon expression level in a single cell was not correlated with Ad doses used. The data indicated that Ad infection with a greater dose increased cell numbers infected but did not enhance the viral gene expression levels in each cell. The levels of viral genes expressed in a single cell were thus relatively constant or limited, which was not revealed by a protein blot analysis. The flow cytometry also has a limited ability to estimate number of infectious viral particles since viral particle numbers and the gene expression levels were not directly correlated.

We also showed that image cytometry detected an expression profile of cyclin E and phosphorylated histone H3 A, and indicated that the technique was widely applicable with different cells and with different types of replication-competent Ad. A dual image cytometric

technique therefore is useful to analyze expression profiles at one cell level, which gives much of quantitative information in comparison with an immunoprecipitation-Western blot method.

Detection of viral gene products with flow cytometry was reported back to 1990s [25] and the techniques was also used to identify Ad-infected cells [26]. Ad vector bearing *green fluorescent protein* gene expanded utility of a cytometric analysis to identify the virus-infected cells [27]. Moreover, a previous study compared sensitivity and utility of a cytometric technique with other methods such as a quantitative polymerase chain reaction, and demonstrated an advantage of detecting E1A and hexon with flow cytometry over the other procedures [28]. An application of recombinant Ad for an anti-cancer agent further augmented values of molecular imaging with a fluorescent dye in terms of detection of target cells and estimation of infectivity [29–31]. We showed in the present study possible benefits of an image cytometric analysis to detect viral and cellular gene products for analysis of Ad infectivity and for prediction of the cytotoxicity. A meticulous sample processing technique is required to analyze protein expression in a clinical setting since the tumor specimens are mixture of tumor cells and stroma, and often contain dead cells. Image cytometry can detect respective proteins expressed on target cells with easy by gating out non-tumorous and dead cells with appropriate Ab. Detection of multiple gene products with different color dyes, which are now available, makes it possible to analyze complexity of interaction between viral and host cell proteins.

Conclusions

Image cytometry is a simple and precise assay method to detect viral and cellular proteins at a single cell level. It requires small cell numbers and is useful for detailed analysis of viral infection processes and cellular responses to them. The technique can also be useful for investigating the expression profiles in a time-dependent manner.

Additional file

Additional file 1: Detailed information as for Ad construction. (DOCX 43 kb)

Abbreviations

Ab: Antibody; Ad: Adenoviruses; AdF35: Adenovirus vector bearing the type-35-derived fiber-knob structure; AdF35/LacZ: AdF35 expressing the β -galactosidase gene; CAR: Coxsachie adenovirus receptor; MK: Midkine; Sur: Survivin; vp: Virus particles; γ -H2AX: γ -H2A histone family member X

Acknowledgments

Not applicable.

Funding

This study was supported by Grants-in-Aid from Japan Society for the Promotion of Science (JSPS KAKENHI Grant number: 26,461,183, 16 K21639, 16 K09598, 17 K10617) and a Grant-in-aid from the Nichias Corporation.

Availability of data and materials

All the data and materials are available upon the requests.

Authors' contributions

TM, TTTN, BZ, MH and MS conducted experiments, IS and YT analyzed the data, KT, HS, KH organized the experiments, and MT prepared the manuscript. All authors read and approved the final manuscript.

Ethics approval and consent to participate

This article does not contain any studies with human beings or animals.

Consent for publication

Not applicable. This article does not contain any studies with human beings or animals.

Competing interests

The authors declare that there is no conflict of interests in this research. We obtained a grant from Nichias Corporation. It is not a pharmaceutical company but a company making industrial products for building, automobiles and pipes (see <http://www.nichias.co.jp/>). The grant is as a kind of their mécénat activities, corporate social contributions, which is aimed to assist for medical research for intractable cancer treatments. We are thereby irrelevant to any employment, consultancy, patents or products in development or marketed products to the company. All the authors agree to publish the data included in the manuscript.

Publisher's Note

Springer Nature remains neutral with regard to jurisdictional claims in published maps and institutional affiliations.

Author details

¹Division of Pathology and Cell Therapy, Chiba Cancer Center Research Institute, 666-2 Nitona, Chuo-ku, Chiba 260-8717, Japan. ²Department of Molecular Biology and Oncology, Graduate School of Medicine, Chiba University, Chiba, Japan. ³Division of Respirology, Chiba Cancer Center, Chiba, Japan. ⁴Department of Medical Oncology, Faculty of Medicine, University of Tsukuba, Tsukuba, Japan. ⁵Department of Respirology, Graduate School of Medicine, Chiba University, Chiba, Japan. ⁶Department of Surgery, School of Medicine, Toho University, Tokyo, Japan. ⁷Department of Pathology, Tokyo Women's Medical University Yachiyo Medical Center, Yachiyo, Japan.

Received: 4 June 2017 Accepted: 31 October 2017

Published online: 10 November 2017

References

- Park GT, Choi KC. Advanced new strategies for metastatic cancer treatment by therapeutic stem cells and oncolytic virotherapy. *Oncotarget*. 2016;7:58684–95.
- Grigg C, Blake Z, Gartrell R, Sacher A, Taback B, Saenger Y. Talimogene laherparepvec (T-Vec) for the treatment of melanoma and other cancers. *Semin Oncol*. 2016;43:638–46.
- Wold WS, Toth K. Adenovirus vectors for gene therapy, vaccination and cancer gene therapy. *Curr Gene Ther*. 2013;13:421–33.
- Zhu ZB, Chen Y, Makhija SK, Lu B, Wang M, Rivera AA, Yamamoto M, Wang S, Siegal GP, Curiel DT, McDonald JM. Survivin promoter-based conditionally replicative adenoviruses target cholangiocarcinoma. *Int J Oncol*. 2006;29:1319–29.
- Miyauchi M, Yoshida Y, Tada Y, Narita M, Maeda T, Bahar R, Kadomatsu K, Muramatsu T, Matsubara S, Nakagawara A, Sakiyama S, Tagawa M. Expression of herpes simplex virus-thymidine kinase gene controlled by a promoter region of the midkine gene confers selective cytotoxicity to ganciclovir in human carcinoma cells. *Int J Cancer*. 2001;91:723–7.
- Yu L, Hamada K, Namba M, Kadomatsu K, Muramatsu T, Matsubara S, Tagawa M. Midkine promoter-driven suicide gene expression and -mediated adenovirus replication produced cytotoxic effects to immortalized and tumour cells. *Eur J Cancer*. 2004;40:1787–94.
- Shayakhmetov DM, Lieber A. Dependence of adenovirus infectivity on length of the fiber shaft domain. *J Virol*. 2000;74:10274–86.
- Sharma A, Li X, Bangari DS, Mittal SK. Adenovirus receptors and their implications in gene delivery. *Virus Res*. 2009;143:184–94.
- Ni S, Gaggar A, Di Paolo N, Li ZY, Liu Y, Strauss R, Sovo P, Morihara J, Feng Q, Kiviati N, Touré P, Sow PS, Lieber A. Evaluation of adenovirus vectors containing serotype 35 fibers for tumor targeting. *Cancer Gene Ther*. 2006;13:1072–81.
- Kim SY, Kang S, Song JJ, Kim JH. The effectiveness of the oncolytic activity induced by Ad5/F35 adenoviral vector is dependent on the cumulative cellular conditions of survival and autophagy. *Int J Oncol*. 2013;42:1337–48.
- Anderson BD, Nakamura T, Russell SJ, Peng KW. High CD46 receptor density determines preferential killing of tumor cells by oncolytic measles virus. *Cancer Res*. 2004;64:4919–26.
- Yu L, Takenobu H, Shimozato O, Kawamura K, Nimura Y, Seki N, Uzawa K, Tanzawa H, Shimada H, Ochiai T, Tagawa M. Increased infectivity of adenovirus type 5 bearing type 11 or type 35 fibers to human esophageal and oral carcinoma cells. *Oncol Rep*. 2005;14:831–5.
- Suzuki T, Kawamura K, Li Q, Okamoto S, Tada Y, Tatsumi K, Shimada H, Hiroshima K, Yamaguchi N, Tagawa M. Mesenchymal stem cells are efficiently transduced with adenoviruses bearing type 35-derived fibers and the transduced cells with the IL-28A gene produces cytotoxicity to lung carcinoma cells co-cultured. *BMC Cancer*. 2014;14:713.
- Bressy C, Benihoud K. Association of oncolytic adenoviruses with chemotherapies: an overview and future directions. *Biochem Pharmacol*. 2014;90:97–106.
- Hasei J, Sasaki T, Tazawa H, Osaki S, Yamakawa Y, Kunisada T, Yoshida A, Hashimoto Y, Onishi T, Uno F, Kagawa S, Urata Y, Ozaki T, Fujiwara T. Dual programmed cell death pathways induced by p53 transactivation overcome resistance to oncolytic adenovirus in human osteosarcoma cells. *Mol Cancer Ther*. 2013;12:314–25.
- Toth K, Lee SR, Ying B, Spencer JF, Tollefson AE, Sagartz JE, Kong IK, Wang Z, Wold WS. STAT2 knockout Syrian hamsters support enhanced replication and pathogenicity of human adenovirus, revealing an important role of type I interferon response in viral control. *PLoS Pathog*. 2015;11:e1005084.
- Yamauchi S, Kawamura K, Okamoto S, Morinaga T, Jiang Y, Shingyoji M, Sekine I, Kubo S, Tada Y, Tatsumi K, Shimada H, Hiroshima K, Tagawa M. Replication-competent adenoviruses with the type 35-derived fiber-knob region achieve reactive oxygen species-dependent cytotoxicity and produce greater toxicity than those with the type 5-derived region in pancreatic carcinoma. *Apoptosis*. 2015;20:1587–98.
- Mittereder N, March KL, Trapnell BC. Evaluation of the concentration and bioactivity of adenovirus vectors for gene therapy. *J Virol*. 1996;70:7498–509.
- Strober W. Trypan blue exclusion test of cell viability. *Curr Protoc Immunol*. 2015;111:Appendix3B 1–3.
- Laemmli UK. Cleavage of structural proteins during the assembly of the head of bacteriophage T4. *Nature*. 1970;227:680–5.
- Carson CT, Schwartz RA, Stracker TH, Lilley CE, Lee DV, Weitzman MD. The Mre11 complex is required for ATM activation and the G2/M checkpoint. *EMBO J*. 2003;22:6610–20.
- Di Marzo D, Forte IM, Indovina P, Di Gennaro E, Rizzo V, Giorgi F, Mattioli E, Iannuzzi CA, Budillon A, Giordano A, Pentimalli F. Pharmacological targeting of p53 through RITA is an effective antitumoral strategy for malignant pleural mesothelioma. *Cell Cycle*. 2014;13:652–65.
- Cheng PH, Rao XM, McMasters KM, Zhou HS. Molecular basis for viral selective replication in cancer cells: activation of CDK2 by adenovirus-induced cyclin E. *PLoS One*. 2013;8:e57340.
- Turner RL, Groitl P, Dobner T, Ornelles DA. Adenovirus replaces mitotic checkpoint controls. *J Virol*. 2015;89:5083–96.
- Eyler YL, Lantz LM, Lewis AM Jr. Flow cytometric detection of DNA tumor virus nuclear oncogene products in unfixed cells: saponin FACS of viral oncogene products. *J Virol Methods*. 1994;46:23–7.
- Weaver LS, Kadan MJ. Evaluation of adenoviral vectors by flow cytometry. *Methods*. 2000;21:297–312.
- Richman L, Meylan PR, Munoz M, Pinaud S, Mirkovitch. An adenovirus-based fluorescent reporter vector to identify and isolate HIV-infected cells. *J Virol Methods*. 2002;99:9–21.
- Li D, He M, Jiang SC. Detection of infectious adenoviruses in environmental waters by fluorescence-activated cell sorting assay. *Appl Environ Microbiol*. 2010;76:1442–8.
- Maida Y, Kyo S, Sakaguchi J, Mizumoto Y, Hashimoto M, Mori N, Ikoma T, Nakamura M, Takakura M, Urata Y, Fujiwara T, Inoue M. Diagnostic potential and limitation of imaging cancer cells in cytological samples using telomerase-specific replicative adenovirus. *Int J Oncol*. 2009;34:1549–56.
- Murali A, Kasman L, Voelkel-Johnson C. Adenoviral infectivity of exfoliated viable cells in urine: implications for the detection of bladder cancer. *BMC Cancer*. 2011;11:168.
- Tsai YC, Tsai TH, Chang CP, Chen SF, Lee YM, Shyue SK. Linear correlation between average fluorescence intensity of green fluorescent protein and the multiplicity of infection of recombinant adenovirus. *J Biomed Sci*. 2015;22:31.